blood

2011 118: 5652-5663
Prepublished online September 27, 2011;
doi:10.1182/blood-2011-05-355339

Erythrocyte membrane changes of chorea-acanthocytosis are the result of altered Lyn kinase activity

Lucia De Franceschi, Carlo Tomelleri, Alessandro Matte, Anna Maria Brunati, Petra H. Bovee-Geurts, Mariarita Bertoldi, Edwin Lasonder, Elena Tibaldi, Adrian Danek, Ruth H. Walker, Hans H. Jung, Benedikt Bader, Angela Siciliano, Emanuela Ferru, Narla Mohandas and Giel J. C. G. M. Bosman

Blood (print ISSN 0006-4971, online ISSN 1528-0020), is published weekly by the American Society of Hematology, 2021 L St, NW, Suite 900, Washington DC 20036.

Erythrocyte membrane changes of chorea-acanthocytosis are the result of altered Lyn kinase activity

Lucia De Franceschi,[1] *Carlo Tomelleri,[1] *Alessandro Matte,[1] Anna Maria Brunati,[2] Petra H. Bovee-Geurts,[3] Mariarita Bertoldi,[4] Edwin Lasonder,[5] Elena Tibaldi,[2] Adrian Danek,[6] Ruth H. Walker,[7,8] Hans H. Jung,[9] Benedikt Bader,[6] Angela Siciliano,[1] Emanuela Ferru,[1,10] Narla Mohandas,[11] and Giel J. C. G. M. Bosman[3]

[1]Department of Medicine, University of Verona, Verona; Italy; [2]Department of Biochemistry, University of Padova, Padova, Italy; [3]Department of Biochemistry and Nijmegen Centre for Molecular Life Sciences, Radboud University Nijmegen Medical Centre, Nijmegen, The Netherlands; [4]Department of Life and Reproduction Sciences, Section of Biochemistry, University of Verona, Verona, Italy; [5]Centre for Molecular and Biomolecular Informatics, Nijmegen Centre for Molecular Life Sciences, Radboud University Nijmegen Medical Centre, Nijmegen, The Netherlands; [6]Department of Neurology, Ludwig Maximilians Universität, Munich, Germany; [7]Department of Neurology, James J. Peters Veterans Administration Medical Center, Bronx, NY and [8]Mount Sinai School of Medicine, New York, NY; [9]University Hospital of Zurich, Zurich, Switzerland; [10]Department of Genetic, Biology and Biochemistry, University of Torino, Torino, Italy; and [11]New York Blood Center, New York, NY

Acanthocytic RBCs are a peculiar diagnostic feature of chorea-acanthocytosis (ChAc), a rare autosomal recessive neurodegenerative disorder. Although recent years have witnessed some progress in the molecular characterization of ChAc, the mechanism(s) responsible for generation of acanthocytes in ChAc is largely unknown. As the membrane protein composition of ChAc RBCs is similar to that of normal RBCs, we evaluated the tyrosine (Tyr)–phosphorylation profile of RBCs using comparative proteomics. Increased Tyr phosphorylation state of several membrane proteins, including band 3, β-spectrin, and adducin, was noted in ChAc RBCs. In particular, band 3 was highly phosphorylated on the Tyr-904 residue, a functional target of Lyn, but not on Tyr-8, a functional target of Syk. In ChAc RBCs, band 3 Tyr phosphorylation by Lyn was independent of the canonical Syk-mediated pathway. The ChAc-associated alterations in RBC membrane protein organization appear to be the result of increased Tyr phosphorylation leading to altered linkage of band 3 to the junctional complexes involved in anchoring the membrane to the cytoskeleton as supported by coimmunoprecipitation of β-adducin with band 3 only in ChAc RBC-membrane treated with the Lyn-inhibitor PP2. We propose this altered association between membrane skeleton and membrane proteins as novel mechanism in the generation of acanthocytes in ChAc. (*Blood*. 2011;118(20):5652-5663)

Introduction

Chorea-acanthocytosis (ChAc) is a rare autosomal recessive neurodegenerative disorder of the neuroacanthocytosis group.[1-3] ChAc is characterized by a neurodegeneration of the basal ganglia, which is associated with the presence of acanthocytes, abnormal erythrocytes with thorn-like protrusions, in the peripheral circulation.[1-3] Molecular studies have identified mutation(s) of the *VPS13A* gene (chromosome 9), encoding a 360-kDa protein chorein of unknown function that is ubiquitously expressed in the brain.[2,4-6] To date, 92 mutations on the *VPS13A* gene have been reported, resulting in low or absent synthesis of chorein or in expression of a functionally defective protein at normal levels.[2,4-6] Chorein has been detected in mature RBCs but it is partially or completely absent in RBCs from patients with ChAc.[6] Because of the lack of knowledge on the structure of chorein and on its interaction with other proteins, we can only speculate on the role of chorein in RBC homeostasis.

In the RBC membrane, 2 major multiprotein complexes bridge the lipid bilayer with the integral membrane proteins to the spectrin-actin cytoskeleton: the ankyrin complex and the junctional or 4.1R complex.[7] Electron microscopy of ChAc RBCs reveals ultrastructural abnormalities in the membrane skeleton as indicated by a heterogeneous distribution of the cytoskeleton. Condensed skeletal structures around protrusions and a less filamentous structure in some large membrane patches indicate a perturbation of membrane cytoskeleton network associated with the membrane protrusions that characterize acanthocytes.[8] These structural data were also supported by the observation that ChAc patients have a fraction of dense RBCs containing acanthocytes with a reduced cell K^+ content compared with normal controls.[9] RBCs from ChAc patients did not show overall abnormalities in RBC membrane protein composition and content, although there is accumulating evidence for neuroacanthocytosis-specific abnormalities in band 3 structure and function.[10] Increased membrane serine-threonine phosphorylation levels, mainly of band 3 and spectrin, increased levels of band 3 tyrosine (Tyr) phosphorylation, and increased activity of membrane-associated casein-kinase has also been described in ChAc RBCs.[11] Increased amounts of N^{ϵ} (γ-glutamyl) lysine isopeptides associated with the RBC membrane have also been reported in a few ChAc patients, indicating a possible perturbation of the anchoring bridges between the membrane and the cytoskeleton.[12,13] There are no consistent data indicating a

Submitted May 17, 2011; accepted September 7, 2011. Prepublished online as *Blood* First Edition paper, September 27, 2011; DOI 10.1182/blood-2011-05-355339.

*C.T. and A.M. contributed equally to this study.

The online version of this article contains a data supplement.

The publication costs of this article were defrayed in part by page charge payment. Therefore, and solely to indicate this fact, this article is hereby marked "advertisement" in accordance with 18 USC section 1734.

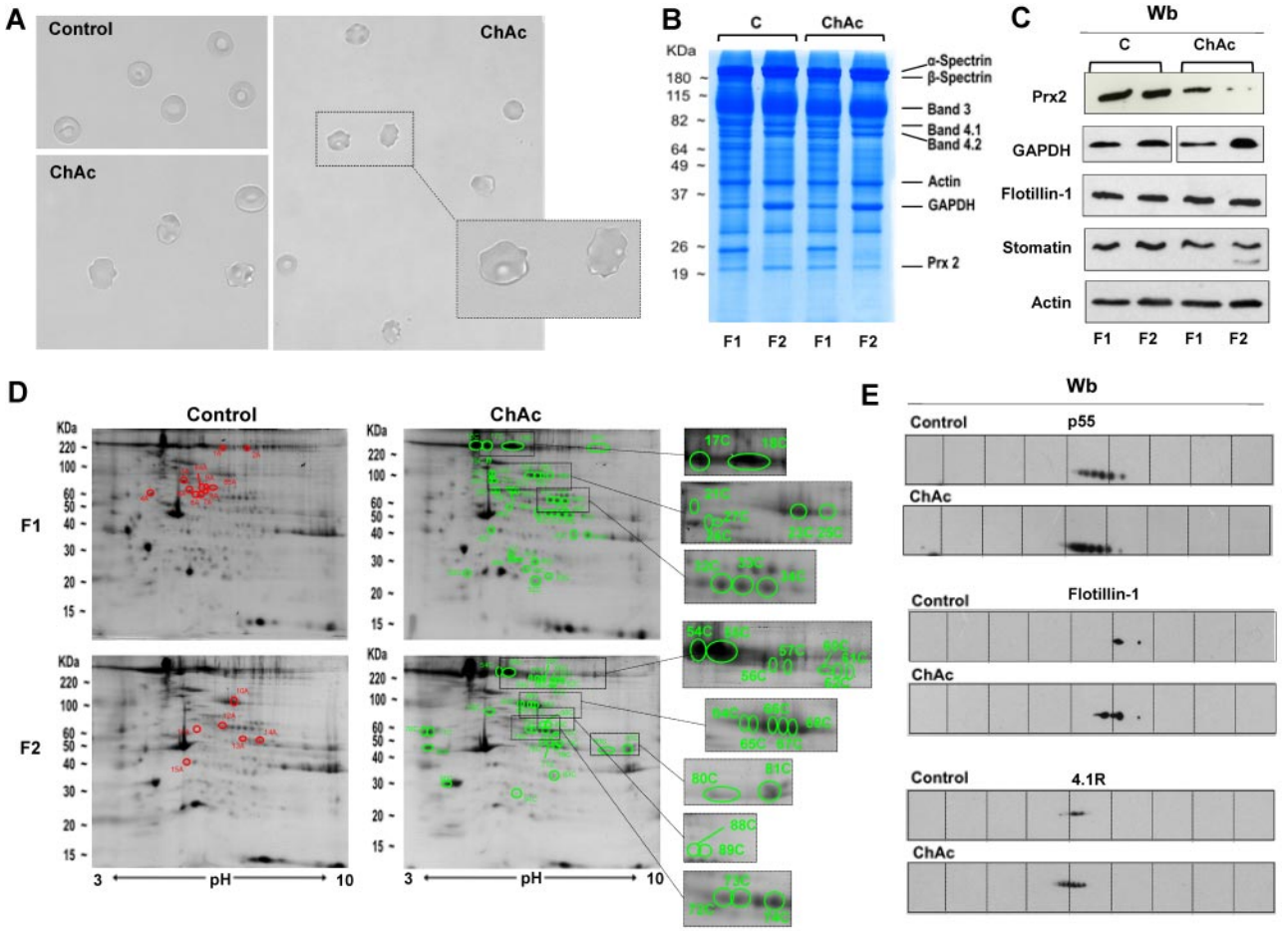

Figure 1. Proteomic analysis of RBC membrane fractions shows differences in ChAc compared with healthy controls. (A) Morphology of RBCs from control and ChAc subjects. (B-E) RBCs from control (C) and ChAc were fractionated in fraction 1 (F1) corresponding to a density < 1.074, containing reticulocytes, and fraction 2 (F2) corresponding to a density > 1.092, containing acanthocytes. (B) The fractionated RBC membrane proteins were separated by 1DE and stained with colloidal Coomassie blue. The bands that were identified by mass spectrometry are indicated: β-spectrin (accession no. P11277), 48% coverage; β-spectrin (accession no. P02549), 52% coverage; band 3 (accession no. P027330), 25% coverage; band 4.1R (accession no. P11171), 22% coverage; band 4.2 (accession no. P16452), 18% coverage; β-actin (accession no. P60709), 26% coverage; GAPDH (accession no. P04406), 18% coverage; and Prx-2 (accession no. P32119), 32% coverage. The figure shows a representative of 9 experiments performed with similar results. (C) Western blot (Wb) analysis of RBC membranes separated by 1DE with specific antibodies against Prx-2, GAPDH, flotillin-1, and stomatin proteins of fractionated RBCs from controls (C) and ChAc subjects. Actin was used as loading control. The data are representative for 8 experiments. (D-E) The membrane proteins of fractionated RBCs (see "Study design") were separated by 2DE. Twin 2DE gels were run: one stained with colloidal Coomassie and the other transferred to membrane for Western blot analysis. (D) The colloidal Coomassie blue–stained gels underwent image analysis, and differently expressed proteins were identified by mass spectrometry (see "Comparative proteomic analysis"; supplemental Methods). Red and green spots indicated the differently expressed proteins based on image analysis. The identified proteins are reported in supplemental Table 2. The figures show 1 representative experiment from a total 8 experiments performed. (E) Western blot (Wb) analysis of the 2DE maps with specific anti–protein p55 antibody on F1 RBCs from control and ChAc subjects (validating the differently expressed spots 32C, 33C, and 34C in panel 1D and supplemental Table 2), anti–flotillin-1 antibody on F1 RBCs from control and ChAc subjects (validating the differently expressed spots 40C in panel D and supplemental Table 2), and anti–protein 4.1R antibody on F2 RBCs from control and ChAc subjects (validating the differently expressed spots 64C-68C in panel D and supplemental Table 2). The figures show one representative experiment of 3 experiments performed with similar results.

relation between lipid content and/or composition and acanthocytosis in ChAc patients.

The recent development of proteomic techniques has yielded a description of RBC membrane proteome, mainly in normal RBCs.[14-18] We used comparative proteomics to study membrane proteome of RBCs from patients with ChAc in relation to normal controls. Differences between normal and ChAc RBCs included changes in Tyr phosphorylation state of band 3, β-spectrin, and other members of the anchoring complexes in ChAc RBCs. We also found abnormal activation of Lyn, a Tyr-kinase of the Src family, independent from its canonical signaling pathway involving primary phosphorylation of Syk. These finding suggest that altered phosphorylation of band 3 and membrane skeletal proteins may play a role in the development of acanthocyte morphology in ChAc.

Methods

Study design

We studied 9 patients with ChAc based on clinical neurologic manifestations, presence of acanthocytes (Figure 1A), and confirmation by either immunoblot analysis for chorein and/or molecular analysis for *VPS13A* mutations as previously described.[6] The demographic and molecular data of patients are reported in Table 1. Blood was obtained by venipuncture using EDTA as an anticoagulant, according to the guidelines approved by the local Ethics Committees for human subject studies of all participating institutions involved. Blood samples (ChAc patients and healthy control donors) were shipped to Verona and Nijmegen at 4°C and processed immediately after arrival. Erythrocytes were isolated from whole blood after removal of white blood cells and platelets as previously described.[19] Because ChAc patients have a dense fraction of RBCs

Table 1. Demographic and molecular data of control and ChAc subjects

	Sex	Age, y	Molecular defect/WB analysis for chorein
Controls (n = 12)	9 females/3 males	35.6 ± 2.3	
ChAc 1	Female	35	Intron 3: c.188–5T > G (splice site); mutation on other allele unknown/ND
ChAc 2	Female	34	ND/chorein absent
ChAc 3	Female	30	Exon 37: c.4286G > C;p.A1428P; intron 55: c.7806G > A;p.P2602P (splice site)/chorein absent
ChAc 4	Female	40	Exon 34: c.3889C > T; p.R1297X; exon 36: c.4216del; p.V1406CfsX20/ND
ChAc 5	Male	47	Intron 22: c.2288 + 2T > C; (splice site mutation); intron 61: c.8472–1G > C; (splice site mutation)/ND
ChAc 6	Female	56	(homozygous) Exon 13: c.1115del; p.K372SfsX2/ND
ChAc 7	Male	32	ND/chorein absent
ChAc 8	Female	38	Intron 6: c.495 + 5G > A (splice site mutation); exon 40: c.4903_4906del; p.K1635VfsX6/ND
ChAc 9	Female	40	ND/chorein absent

WB indicates Western blot; and ND, not determined.

enriched in acanthocytes,[9] we analyzed RBCs separately according to RBC density.

For semiquantitative proteome analyses, we separated the RBCs in 1 of 2 ways. Cells were separated into 5 fractions (I-V) based on volume and density using counter flow centrifugation followed by Percoll gradient centrifugation, with fraction I containing the youngest and fraction V the oldest erythrocytes and acanthocytes. The membrane proteomes of these fractions were analyzed as described previously.[15]

Alternatively, RBCs were separated into 2 fractions: fraction 1 (F1) corresponding to a density < 1.074, containing reticulocytes, and fraction 2 (F2) corresponding to a density > 1.092, containing acanthocytes, for proteomic analysis by 2-dimensional electrophoresis matrix-assisted laser desorption/ionization time-of-flight mass spectrometry, which requires a relatively large amount of proteins for the analysis.[19,20] Where indicated, control RBCs were incubated in the presence of sodium orthovanadate as previously described by Bordin et al.[21]

RBC morphology, membrane preparation, and membrane cytoskeleton extraction

To study cell morphology, RBCs were fixed as previously described by Matte et al[22] and imaged using a Leica TCS SP5 II microscope equipped with an objective HCX PL APO λ blue 63.0×, NA 1.40 oil.

RBC membrane fractions were obtained by lysing 1 volume of packed cells in 10 volumes of ice-cold phosphate lysis buffer (5mM Na_2HPO_4, pH 8.0, in the presence of protease inhibitors, cocktail tablet, Roche Diagnostics; 3mM benzamidine, 1mM Na_3VO_4). Samples were incubated for 10 minutes on ice and centrifuged for 10 minutes at 12 000*g* at 4°C. Membranes were then washed 4 times by centrifugation at 12 000*g* at 4°C with phosphate lysis buffer until they appeared almost white.[15]

To assess the strength of the interaction between cytoskeleton and the lipid bilayer, cytoskeletal proteins were extracted by resuspending membranes (100 μg of total protein) in 1 mL of 100mM Na_2CO_3, pH 11. The suspension was passed 5 times through a 25-gauge needle, mixed and incubated for 30 minutes at 4°C. Soluble proteins were removed by centrifugation for 30 minutes at 200 000*g*. This procedure was repeated twice. Proteins from pelleted membranes were extracted by either detergent or NaCl. Briefly, packed erythrocyte membranes were incubated for 1 hour at 4°C with 50mM Tris-HCl, pH 7.5, 10% glycerol, 1mM sodium orthovanadate, and protease inhibitor cocktail in the absence or the presence of either 1% Triton X-100[22] or 0.6M NaCl. After ultracentrifugation, the supernatants and precipitates were analyzed by 1-dimensional electrophoresis (1DE) and either stained with colloidal Coomassie or transferred to membranes for immunoblot analysis with the appropriate antibody.[22]

Comparative proteomic analysis

Semiquantitative proteomic analysis. All the analyses were performed essentially as previously described.[15] Details are reported in supplemental Methods (available on the *Blood* Web site; see the Supplemental Materials link at the top of the online article). Samples of various origins were quantified by the label-free peptide counting method emPAI, which calculates protein abundance, as has been applied for a quantitative analysis of RBC membranes during storage.[15] Data were normalized using the median emPAI value per sample. This protocol has been shown to result in a reliable identification of all erythrocyte membrane proteins and to enable semiquantification of the major protein species.[15] To be able to apply this method to multiple samples in an efficient and cost-effective manner, we reduced the running time of the SDS-PAGE step and extended the running time of the HPLC gradient from 1.5 to 4 hours. This "one-slice" method yielded 300 to 400 reliably identified proteins, comparable with those found earlier by us and others using one-dimensional as well as 2-dimensional electrophoresis.[15,23,24]

Gel electrophoresis of RBC membrane. For 1DE, RBC membranes were solubilized in sample buffer (50mM Tris, pH 6.8, 100mM β-mercaptoethanol, 2% volume/volume SDS, 10% volume/volume glycerol, a few grains of bromophenol blue), and loaded on to either 8% or 10% polyacrylamide gels. Whenever peroxiredoxin-2 (Prx-2) was evaluated, RBCs were lysed in the presence of NEM (100mM) in the phosphate lysis buffer and solubilized in sample buffer with NEM (100mM).[19,20,22] For 2-dimensional electrophoresis (2DE), RBC membranes were delipidated and separated by 2DE as previously described.[19,20,22] Details are presented in supplemental Methods. After electrophoresis, the gels were stained with colloidal Coomassie followed by image analysis using "Progenesis SameSpots" software (Non Linear Dynamics).[20] Details of image analysis are reported in supplemental Methods. The selected bands or spots were identified by 2DE matrix-assisted laser desorption/ionization time-of-flight mass spectrometry/mass spectrometry analysis (see supplemental Methods for more details).

Immunoblot analysis and dephosphorylation of blotted proteins

Proteins were transferred from 1D or 2D gels to membranes for immunoblot analysis and probed with specific antibodies as previously described[19,20] (see also supplemental Methods for details). Dephosphorylation of blotted proteins was carried out as described in supplemental Methods.

Peptides and recombinant proteins

The phosphopeptide of band 3 (amino acids 1-26) and its unphosphorylated analog were synthesized as described previously.[25] The recombinant GST-Lyn/SH3 domain was expressed and purified according to the protocol described by Trentin et al.[26] The GST-Lyn/SH2 domain was expressed and purified as previously reported.[27]

Phosphorylation of erythrocyte membranes

Erythrocyte membranes (3 μg protein) were phosphorylated for 10 minutes at 30°C in 30 μL of an incubation mixture containing 50mM Tris-HCl, pH

7.5, 10mM $MnCl_2$, 30μM ATP, 200μM sodium orthovanadate, and 15nM of exogenous Lyn Tyr kinase, purified from rat spleen.[27] When required, the phosphorylation assays were carried out in the absence or presence of the GST-Lyn/SH2 domain or the GST-Lyn/SH3 domain, respectively. The solubilized membranes were analyzed by immunoblot with the anti–p-Tyr antibody. The membranes were reprobed with anti–β-actin antibody as a loading control. When indicated, washed RBCs from control and ChAc subjects were incubated with and without the Src family kinase inhibitors PP1 (10μM) and PP2 (10μM) as previously reported.[19,27]

Preparation of Syk-phosphorylated membranes of erythrocytes

Membranes were phosphorylated by 15nM $p36^{Syk}$ for 10 minutes in 50mM Tris-HCl, 10mM $MnCl_2$, 30μM ATP, and 200μM sodium orthovanadate. Syk-phosphorylated membranes were separated from $p36^{Syk}$, ATP, and other reagents by centrifugation and washed twice as previously reported.[27]

Identification of putative phosphorylation targets of Lyn by sequence and structure analyses

The sequences of the different Tyr-phosphorylated proteins were obtained from the NCBI reference sequence database using their accession numbers. They were analyzed by means of the GPS Version 2.0 software to identify putative Lyn target sites.[28] Details are reported in supplemental Methods.

Results

Proteomic analysis of ChAc RBC membranes shows differences compared with membranes from healthy controls

Analysis of ChAc RBC membrane proteins by 1DE followed by protein staining showed that the membrane protein composition of ChAc RBCs was very similar to that of RBCs from healthy controls, except for a band at approximately 20 kDa, which was markedly reduced in the high-density (F2) fraction of RBCs of ChAc patients (Figure 1B). This band was excised from the gel and identified by mass spectrometry as Prx-2. Analysis of the RBC membrane protein composition by comparative semiquantitative proteomic approach showed an enrichment in ChAc RBC membranes for spectrin, ankyrin, and protein 4.2 major component of the ankyrin complex (supplemental Table 1). The concentrations of the raft-associated flotillins did not differ between control and ChAc samples. However, stomatin, another raft-associated protein, was conspicuously enriched in the ChAc samples (supplemental Table 1). The membrane association of GAPDH was variable with an increase in 2 of 3 ChAc patients and a decrease in one ChAc patient (supplemental Table 1). In addition, proteins of the small G protein family were hardly detectable in the control samples but were abundant in the patients' membrane fractions. All membrane samples contained similar amounts of heat shock proteins (data not shown). Immunoblot analysis with specific antibodies confirmed: (1) a reduction of membrane-associated Prx-2 in both low- and high-density fractions of ChAc RBCs compared with controls; (2) an increased membrane association of GAPDH in the high-density fraction of ChAc RBCs that were enriched in acanthocytes compared with normal controls; and (3) a similar membrane content of flotillin 1 in ChAc and control RBCs (Figure 1C).

For a more detailed analysis, we performed 2DE followed by identification of the differently expressed proteins by mass spectrometry. Using a 2-fold abundance as the selection criterion (see "Comparative proteomic analysis"), we detected 50 spots that were differently expressed in high-density fraction (F2) of ChAc RBCs and 41 spots differently expressed in low-density fraction (F1) of ChAc RBCs (Figure 1D; supplemental Table 2). It is to be noted that our protein identifications are in strong accordance with previously published 2DE maps of RBC membrane.[14,20] The identified proteins were divided into 8 functional clusters: I, proteins of the anchoring complexes; II, cytoskeleton proteins; III, raft-related proteins; IV, membrane channels and transporters; V, intracellular signaling proteins; VI, metabolic enzymes; VII, proteins of the ubiquitin-proteasome system; and VIII, stress response proteins and chaperones.[20] We validated the 2DE data by immunoblot analysis of some of the identified proteins: protein p55 in F1 fractionated RBCs, flotillin-1 in F1 fractionated RBCs, and protein 4.1 in F2 fractionated RBCs (Figure 1E). The differences in membrane and cytoskeleton proteins in ChAc RBC observed in 2DE maps were mainly related to protein 2DE mobility shift, possibly reflecting protein post-translational modifications, such as phosphorylation (Figure 1D-E; supplemental Table 2). This is also supported by the similar abundance of membrane and cytoskeleton proteins in 1DE analysis of ChAc and control RBC membranes (Figure 1B).

Differential extraction of membrane proteins reveals differences in membrane organization in ChAc RBCs

To explore putative ChAc-associated changes in membrane organization, we assessed the strength of binding of the major erythrocyte membrane and cytoskeletal proteins to the lipid bilayer by analyzing the proteome after incubation of the membrane fractions with 100mM Na_2CO_3, pH 11 (see "RBC morphology, membrane preparation, and membrane cytoskeleton extraction"). In controls, this alkaline treatment led to the virtual disappearance of most cytoskeletal and membrane-associated proteins, such as spectrin, ankyrin, and GAPDH. This was accompanied by enrichment of most integral membrane proteins, including band 3 and Glut1, and by a large increase in the concentration of stomatin (supplemental Table 3). The loss of GPC, but not GPA, suggests that a considerable fraction of the GPC molecules is extracted together with the cytoskeleton. As in control samples, extraction of ChAc membranes resulted in the depletion of the same proteins as seen in normal membranes and also in enrichment for most integral membrane proteins with band 3 as a notable exception (supplemental Table 3).

Because recent studies have suggested that changes in membrane protein phosphorylation state play an important role in the modulation of RBC membrane protein-protein functional cross-talk and stability of multiprotein structures,[29,30] we studied the Tyr phosphorylation profile of RBC membrane from control and ChAc subjects.

The Tyr-phosphorylation state of ChAc RBC membrane proteins is increased compared with normal controls

Evaluation of the Tyr phosphorylation pattern of RBC membranes from normal and ChAc density-separated RBCs by immunoblot analysis showed a higher Tyr phosphorylation state of various membrane proteins in ChAc RBCs (Figure 2).

The 2DE Tyr-phospho maps confirmed the presence of trains of Tyr-phosphorylated proteins in the gel area corresponding to the differently expressed spots noted in 2DE maps: ankyrin (17-18C in F1 and 54C-57C and 60C-62C in F2 from ChAc RBCs), protein 4.1R (21C, 23C, 25 C in F1 and 64C-68C in F2 from ChAc RBCs), protein p55 (32C-34C in F1 from ChC RBCs) and dematin (88C-89C in F2 from ChAc RBCs; Figure 1D; supplemental Table 2). These data are also supported by the absence of reactivity when

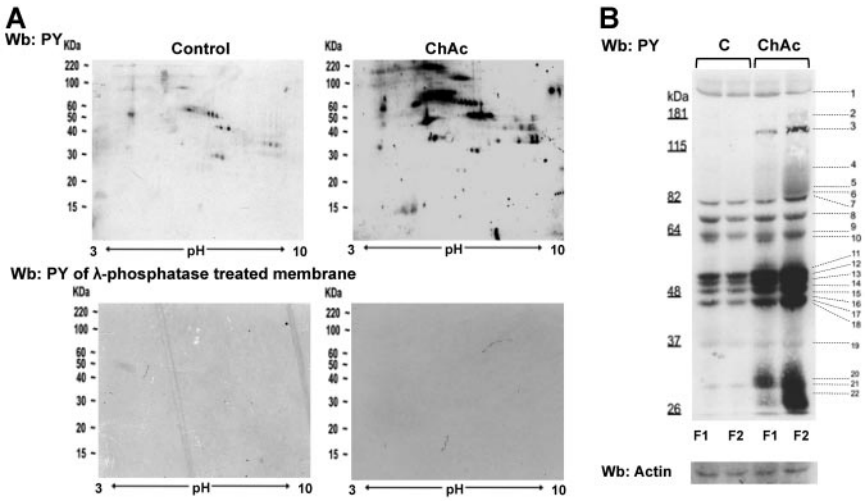

Figure 2. Tyr phosphorylation of RBC membrane protein is increased in ChAc compared with normal controls. RBCs from control (C) and ChAc subjects were fractionated as described in "Study design" and in the legend of Figure 1B-E. Western blot (Wb) analysis with specific anti–phosphotyrosine (PY) antibodies of RBC membrane proteins separated by either bidimensional electrophoresis (2DE) or monodimensional electrophoresis (1DE). (A) Twin 2DE gels were run: one used for colloidal Coomassie-stained gels (Figure 1D) and the other for the Western blot analysis with specific anti–phosphotyrosine (PY) antibodies. Top panel: Membranes of high-density RBC fraction (F2) from control (C) and ChAc subjects. Similar results were also obtained in low-density RBC fraction (F1) from control and ChAc (data not shown). Bottom panel: Dephosphorylation of blotted proteins by recombinant λ protein phosphatase (400 U/mL). The blotted membranes were incubated in TBS containing 1% BSA, 0.1% Triton X-100, 2mM $MnCl_2$ (overnight at 4°C), and then probed with anti–phosphotyrosine antibodies. The data are representative for 3 experiments with similar results. (B) 1DE gels (13 cm) were blotted for Western blot (Wb) analysis with specific anti–phosphotyrosine (PY) antibodies. The bands with different staining intensities were identified by mass spectrometry (Table 2; "Comparative proteomic analysis"; supplemental Methods). Actin was used as a loading control. The data are representative of 8 experiments. See also supplemental Figure 1B for densitometric analysis of the Tyr phosphorylation profile of the RBC membrane proteins.

the membranes were treated with λ-phosphatase, which was used to remove phosphate groups from blotted proteins (Figure 2A bottom panel). The differently Tyr-phosphorylated proteins were excised from the 1D-stained gels and identified by mass spectrometry (Figure 2B). According to their functions, the identified proteins were divided into 8 functional clusters: I, membrane protein, band 3; II, cytoskeleton network proteins β-spectrin and β-actin; III, ankyrin complex proteins, ankyrin, band 4.2; IV, membrane junctional complex proteins, band 4.1, p55, β-adducin; V, intracellular signaling protein; VI, metabolic enzymes, such as GAPDH; VII, stress response proteins, such as catalase; and VIII cell trafficking protein, such as Ras-related proteins (Table 2). Of note, we found a Tyr-phosphorylated β-spectrin fragment in both F1 and F2 fractions from ChAc patients, and we identified a phosphopeptide of β-adducin (R.MLDNLGYR.T) in the dense RBC fraction from ChAc subjects (Table 2). These results

Table 2. Proteins with different degrees of Tyr phosphorylation in RBC membranes from control and ChAc subjects

Band no.	AC	Protein	Theoretical protein MW, kDa	Matching peptide	Coverage, %
1	P11277	β-spectrin (SPTB1)	246.468	146	50
2	P16157	Ankyrin (ANK1)	206.265	20	22
3	Q8WX82	β-I Spectrin form β I σ 3 (fragment; Q8WX82)	117.549	14	20
4	P02730	Band 3 anion transport protein (B3AT)	101.792	16	18
5	P02730	Band 3 anion transport protein (B3AT)	101.792	23	24
6	Q9H4B4	Serine threonine protein kinase PLK3 (PLK3)	71.629	6	8
7	P35612	β-adducin (ADDB)	80.854	9	11
8	P11171	Band 4.1 (EPB41)	97.017	10	24
9	P16452	Band 4.2 (EPB42)	77.009	9	12
10	Q9H4B4	Serine threonine protein kinase PLK3 (PLK3)	71.629	6	11
11	Q00013	55-kDa erythrocyte membrane protein (EM55)	52.296	19	34
12	Q00013	55-kDa erythrocyte membrane protein (EM55)	52.296	6	18
13	P47895	Aldehyde dehydrogenase family 1 member A3 (AL1A3)	56.108	3	6
14	P04040	Catalase (CATA)	59.756	4	9
15	O94921	Serine threonine protein kinase PFTAIRE-1 (CDK14)	53.057	5	10
16	Q14012	Calcium calmodulin-dependent protein kinase type 1 (KCC1A)	41.337	4	10
17	P60709	β-actin (ACTB)	41.737	10	34
18	Q96GD4	Serine threonine protein kinase 12 (AURKB)	39.311	4	15
19	P04406	Glyceraldehyde-3-P-dehydrogenase (G3P)	36.053	9	36
20	P27105	Stomatin (STOM)	31.731	10	40
21	P00918	Carbonic anhydrase 2 (CAH2)	29.246	3	11
22	Q96E17	Ras-related protein Rab-3C (RAB3C)	25.952	3	17

The corresponding bands are indicated in Figure 2B. The success rate of protein identification by matrix-assisted laser desorption/ionization time-of-flight mass spectrometry/mass spectrometry was 82% ± 6.7% (n = 9).

AC indicates accession number; and MW, molecular weight.

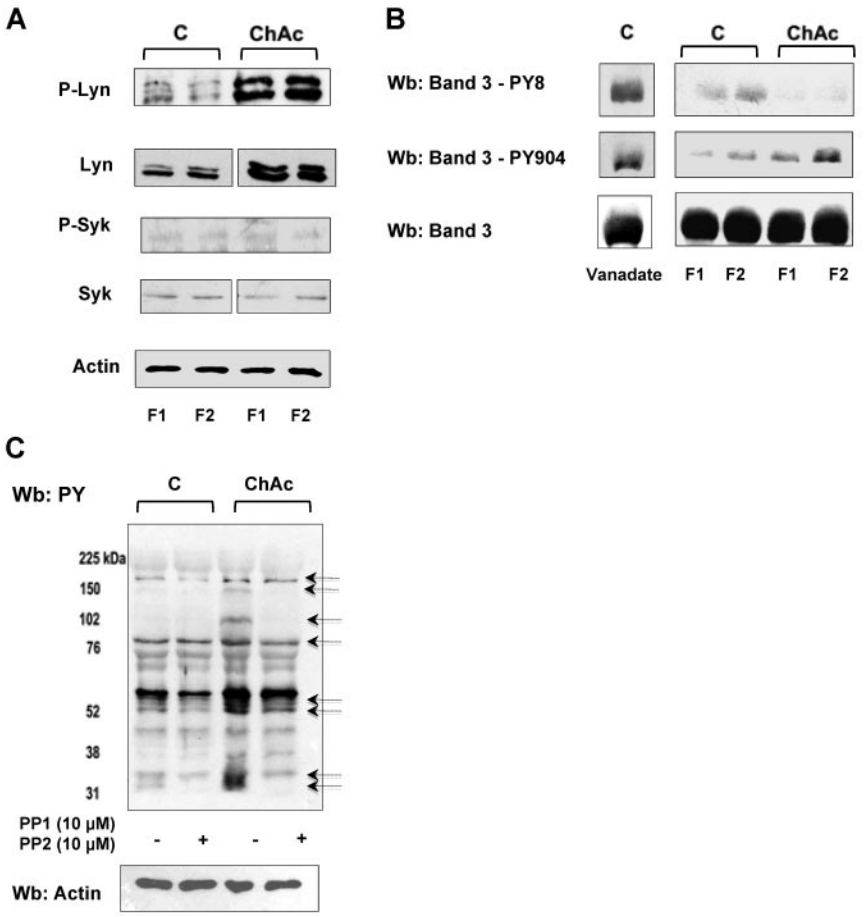

Figure 3. ChAc RBCs show increased Lyn Tyr kinase associated with the membrane. RBCs from control (C) and ChAc were fractionated as described in "Study design" and in the legend of Figure 1B-E. (A) Western blot analysis with specific antibodies of membrane-associated Tyr kinase Lyn and phospho-Lyn (p-Lyn), Syk, and phospho-Syk (p-Syk). Actin was used as a loading control. Shown is a representative of 6 experiments. Vertical line(s) have been inserted to indicate a repositioned gel lane. (B) Western blot (Wb) analysis with specific antibodies against Tyr-8 on the N-terminal of band 3, as a Syk target, and Tyr-904 on the transmembrane domain of band 3 (as a Lyn target). We used normal RBCs treated with Na-vanadate (see "Study design") as positive controls. Total band 3 was used as loading control. (C) Western blot (Wb) analysis with specific anti–phosphotyrosine (PY) antibodies of high-density fraction (F2) of RBCs from control (C) and ChAc subjects are shown. The F2 RBCs were incubated with or without the Src family kinase inhibitors PP1 (10μM) and PP2 (10μM) as previously reported.[19] The arrows indicated the bands affected by PP1-PP2 treatment in ChAc RBCs compared with untreated ChAc RBCs. The data are representative of 3 experiments (on 6-cm gels). Actin was used as a loading control. The data are representative of 3 experiments. Similar results were also obtained with cells from low density fraction (F1) control and ChAc RBCs (data not shown).

suggest that altered phosphorylation may contribute to acanthocytosis in ChAc.

Lyn is abnormally activated in ChAc RBCs and is independent from Syk sequential phosphorylation

Because Tyr-kinase Syk and the Src family kinase Lyn have been described as being involved in modulating band 3 function in healthy RBCs,[27] we studied membrane association of Syk and Lyn in control and ChAc erythrocytes.

In both F1 and F2 RBCs from ChAc patients, we observed an increased membrane association of active Lyn (phospho-Lyn, Figure 3A). In contrast, the amount of membrane-bound total and active Syk (phospho-Syk) was almost undetectable in ChAc and barely detectable in control RBCs (Figure 3A). We previously reported a sequential phosphorylation of band 3 catalyzed by the concerted action of Syk and Lyn, with Tyr-8 and Tyr-21 being first targeted by Syk and thereby serving as docking sites for the Src homology domain 2 (SH2) of Lyn. Lyn, once recruited, phosphorylates Tyr-359 and Tyr-904 of band 3[27] as well as other proteins, such as spectrins and adducin (unpublished data).

We used specific antibodies against Tyr-8 on the N-terminal of band 3, as a Syk target, and Tyr-904 on the transmembrane domain of band 3, as a Lyn target. We found increased Tyr phosphorylation at Tyr-904 compared with normal RBCs (Figure 3B). Phosphorylation of residue Tyr-8 was almost absent in both fractions from ChAc RBCs and only slightly detectable in normal RBCs. Since we have previously reported that activated Syk might be present in the cytoplasm in a truncated form,[21] we evaluated Syk activity in the cytoplasm. Syk activity was similar in the cytoplasm of normal and ChAc RBCs (data not shown), suggesting a peculiar membrane recruitment of Lyn to ChAc membranes that occurs independent of preceding phosphorylation of band 3 by Syk.

To evaluate whether the Tyr-phospho profile of ChAc RBC membrane might be affected by in vitro Lyn inhibition, we incubated control and ChAc RBCs with both PP1 and PP2, Src family kinase inhibitors, to obtain a more stable inhibition of kinase activity. As shown in Figure 3C, in ChAc RBCs the PP1/PP2 treatment markedly reduced Tyr-phosphorylation state of several bands, including band 3, thus supporting the role of Src kinase as determinant of the peculiar ChAc RBC membrane Tyr-phosphorylation profile.

Because the amount of Lyn was markedly higher in ChAc erythrocytes than in control RBCs, we characterized Lyn RBC membrane association. Lyn was almost entirely solubilized by the treatment with Triton-X 100 in both control and ChAc RBCs (Figure 4A lanes 2 and 3 and lanes 7 and 8). However, treatment with high ionic strength medium (0.6M NaCl, see "Study design") resulted in remarkably increased extraction of Lyn from ChAc RBC membranes compared with that from membranes of control cells, accounting for the increased Lyn concentration (Figure 4A lanes 4 and 5 vs lanes 9 and 10). These data suggest there are several pools of Lyn in ChAc RBCs, which associate with the membrane by multiple modes. This is corroborated by the observation that a fraction of Lyn was released from ChAc RBC membranes by agents capable of disrupting the SH2 domain/phospho-Tyr interaction, such as GST-Lyn/SH2 and the phosphorylated NH2 terminus of band 3 (Figure 4B).

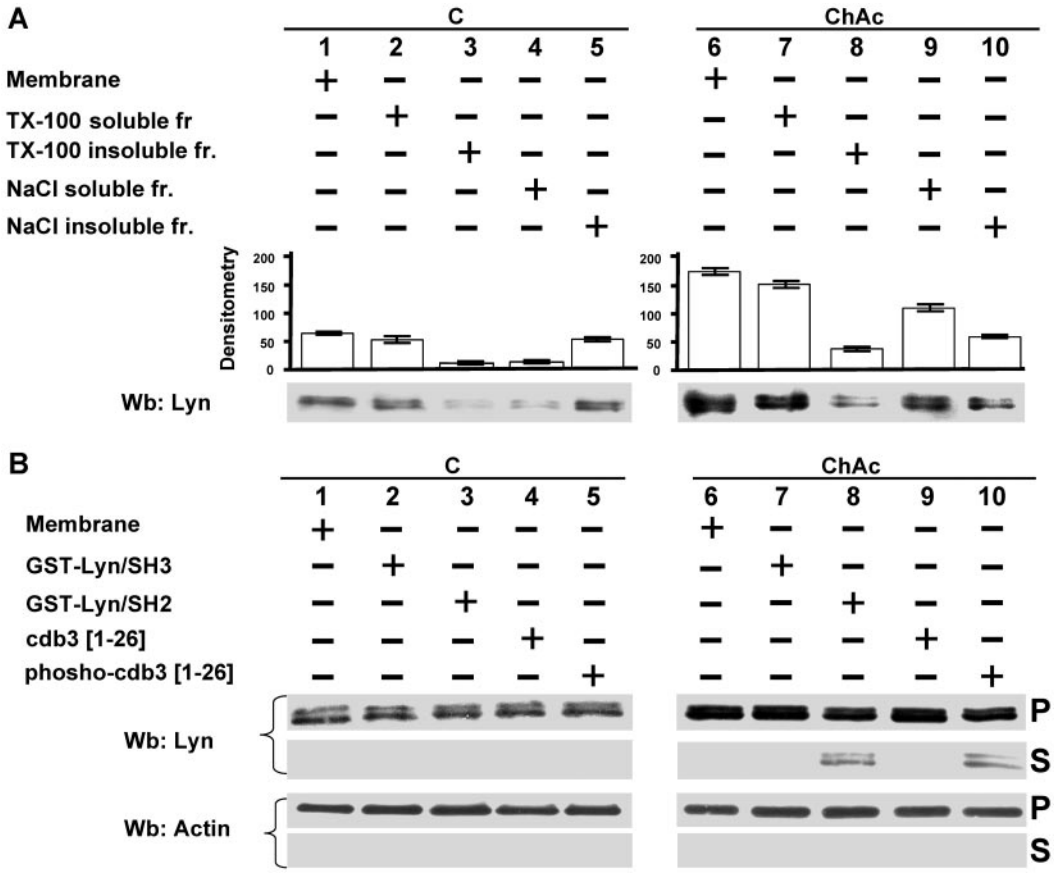

Figure 4. Modes of interaction of Lyn with membranes from ChAc RBCs. (A) Membranes of F2 RBCs from control (C) and ChAc subjects were extracted with Triton X-100 or NaCl (see "RBC morphology, membrane preparation, and membrane cytoskeleton extraction") and assayed after ultracentrifugation for the presence of Lyn by Western blot (Wb) analysis. The data shown here are obtained with F2 ChAc RBCs. Similar data were obtained with F1 control and ChAc RBCs (data not shown). (B) Membranes of F2 RBCs from control (C) and ChAc subjects were incubated in the presence or absence of GST-Lyn/SH3, GST-Lyn/SH2, cdb3, or phospho (p)–cdb3 and assayed after ultracentrifugation for Lyn in the resulting soluble (S) and pellet (P) fractions for the presence of Lyn by Western blot (Wb) analysis. Similar data were obtained from F1 control and ChAc RBCs (data not shown). The membranes were reprobed with anti–actin antibody as loading control.

Exogenous Lyn phosphorylates several targets in ChAC RBC membrane independent of Syk

We then evaluated whether in ChAc RBCs the ability of Lyn to phosphorylate RBC membrane proteins in vitro was still dependent on a Syk-related mechanism. Preparations from control and ChAc RBC membranes were washed free of the phosphatase inhibitor vanadate and resealed with exogenous Lyn in the presence and absence of GST-Lyn/SH2 and GST-Lyn/SH3 domains. Exogenous Lyn was shown to phosphorylate ChAc membrane proteins much more efficiently than control fractions (Figure 5). In addition, the Tyr phosphorylation profile remained unaltered in the presence of the GST-Lyn/SH3 domain, with only a slight decrease when the GST-Lyn/SH2 domain was added (Figure 5). These data indicate that the ability of Lyn to Tyr-phosphorylate ChAc membrane proteins is not dependent on a preceding membrane binding and activity of Syk as previously reported for control RBCs.[27] Thus, ChAc-associated alterations in the membrane protein organization may allow Lyn to target its substrates independently from Syk. Interestingly, exogenous Lyn promotes Tyr phosphorylation of membrane proteins other than band 3, similarly to that observed in the naturally occurring Tyr phosphorylation profile of ChAc RBC membranes (Figures 3A and 5). It is of note that in vitro phosphorylation of ChAc RBC membrane by exogenous Lyn involved a smaller number of proteins (bands) at molecular weights lower than 48 kDa compared with intact ChAc RBCs. Otherwise, these proteins showed reduced Tyr phosphorylation in PP1/PP2-treated ChAc RBCs, suggesting that Lyn might be also part of other signaling pathways involving other kinases or play a role as downstream regulator of phosphatase(s) similarly to what we previously described in other RBC models.[31,32]

Bioinformatic analysis of the differentially Tyr-phosphorylated proteins reveals Lyn targets in ChAc RBCs

To evaluate the presence of possible Lyn targets on ChAc RBC membrane proteins differentially Tyr-phosphorylated, we carried out an extensive bioinformatic analysis of putative Lyn target sites in the Tyr-phosphorylated proteins identified. This analysis reveals that approximately 75% of the proteins have at least one highly Lyn-selective site (Table 3). Only 3 of them (aldehyde dehydrogenase, carbonic anhydrase, and glyceraldehyde dehydrogenase) show low specificity and 2 (stomatin and rab) an even lower specificity for Lyn, with increased specificity for other Src kinase members (data not shown). Because we found a highly phosphorylated β-spectrin peptide in the proteomic analysis and also identified a β-adducin phosphopeptide, we carried out a sequence structure analysis of β-spectrin or β-adducin to further characterize the Lyn targets in these 2 proteins. The analysis of the sequence of β-spectrin for Lyn-directed peptides with a high threshold score more than 2.4 identified 5 peptides (Table 3). An intercrossed search to identify whether these peptides could also serve as substrates for Src Tyr kinases restricted the Lyn-specific target

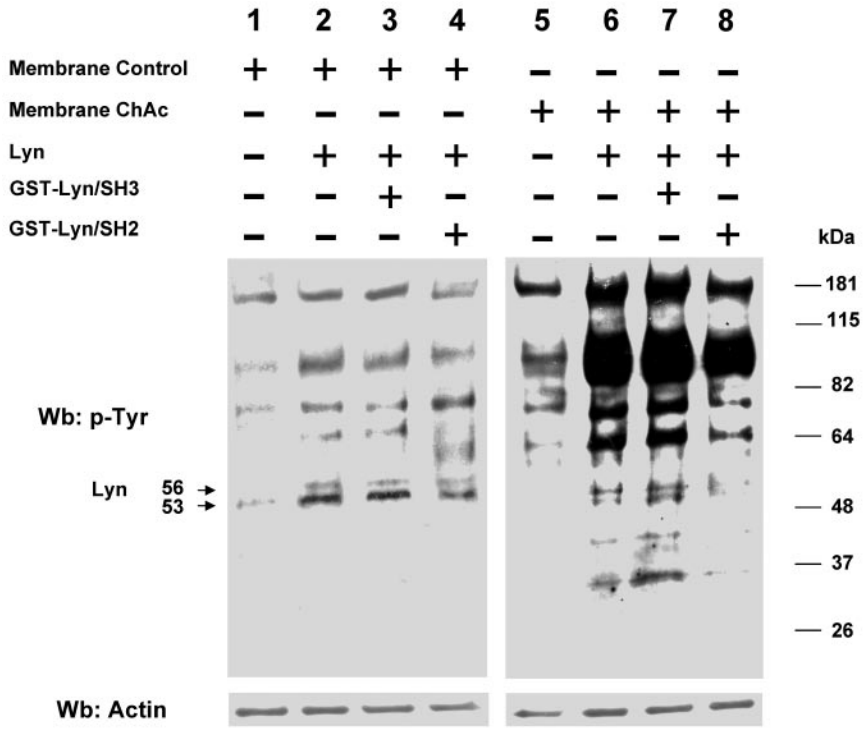

Figure 5. Phosphorylation patterns of normal and ChAc RBC membranes by exogenous Lyn. Membranes of high-density fraction (F2) of RBCs from control (C) and ChAc subjects were incubated without (lanes 1 and 5) or with exogenous Lyn (lanes 2-4 and 6-8) and with GST-Lyn/SH3 (lanes 3 and 7) or GST-Lyn/SH2 (lanes 4 and 8), respectively. Samples were then analyzed by Western blot (Wb) analysis with anti–phosphotyrosine antibodies. Similar data were obtained with F1 control and ChAc RBCs (data not shown). The membranes were reprobed with anti–actin antibody as loading control.

sequences to 2 Tyr residues Tyr-307 and Tyr-1590. Inspection of the 3D structure indicated that the Tyr-307 is located inside the triple-helical bundle, whereas Tyr-1590 is in the linker region preceding repeat 14, at the interface of the ankyrin binding domain (repeats 14 and 15)[33-35] (Table 3). The phosphopeptide of β-adducin (Tyr-377) is a specific target of Lyn with little specificity for Src (Table 3) and is located in a highly conserved sequence of the neck domain of the protein.[36]

Lyn-mediated phosphorylation of ChAc membranes alters the interaction of band 3 with β-adducin

We then evaluated the role of Lyn-dependent phosphorylation of band 3 in the interaction with β-adducin in ChAc RBCs compared with normal erythrocytes. We first phosphorylated band 3 by exogenous Syk with or without exogenous Lyn using normal RBC membranes and then extracted by Triton-X (Figure 6A). The immunoprecipitated band 3 from the resulting extract was further subjected to immunoblot analysis with anti–adducin antibody. As shown in Figure 6B, in control erythrocytes the presence of β-adducin in the band 3 immunoprecipitate was dramatically decreased only if the membranes were sequentially phosphorylated by Syk and Lyn. Because in ChAc RBCs we have shown band 3 Tyr-phosphorylated by Lyn independently from Syk phosphorylation, we immunoprecipitated band 3 from ChAc extracts, and we observed a small amount of β-adducin coimmunoprecipitated. This increased further when membranes were incubated in the presence of the Src kinase inhibitor PP2, suggesting that the altered Lyn activity was implicated in the mechanism of association between band 3 and β-adducin in ChAc RBCs.

Discussion

An integrated proteomic approach enabled us to analyze the perturbation of membrane protein organization in ChAc RBCs at the molecular level. Our analysis indicated that this membrane perturbation mainly affects the multiprotein complexes that anchor the cytoskeleton to the membrane through band 3. The ChAc-related alterations in the membrane association of GAPDH and hemoglobin also suggest a perturbation of their binding sites on band 3. These observations are in agreement with the reduction in association of Prx-2 with the membrane, which may be the result of unavailability of the Prx-2 docking site on band 3, as has also been reported in β-thalassemic RBCs.[22] These data confirm and extend previous observations of neuroacanthocytosis-associated alterations on band 3[10] and extend these to ChAc-specific alterations in band 3 function.

Previous studies have shown that the Tyr phosphorylation state of RBC membrane proteins is involved in regulation of membrane cohesion and mechanical stability.[29] Accordingly, we found that several membrane proteins are highly Tyr-phosphorylated in ChAc RBCs compared with controls. These proteins are band 3 and other components of the 2 anchoring complexes. Because band 3 is part of both complexes, these findings suggest that phosphorylation-induced perturbation of protein-protein interactions may be centered on band 3. Changes in the protein phosphorylation state can modify protein-protein interactions and thereby multiprotein complex formation and/or functions.[37,38]

Previous studies documented that the Syk-Lyn signaling pathway working in concert can modify band 3 function in healthy RBCs.[27] It is noteworthy that we found increased association of active Lyn with the ChAc membranes in the absence of Syk. This is surprising because Syk is responsible for the primary Tyr phosphorylation of band 3 that precedes membrane recruitment of Lyn in normal RBCs.[27] In ChAc membranes, the membrane-associated form of Lyn was normally solubilized by detergent but differentially partitioned by ionic strength extraction. These data point toward a contribution of electrostatic interactions in Lyn binding and suggest the existence of different pools of Lyn associated with the membrane. A small amount of Lyn was displaced from the

Table 3. Bioinformatic analysis of the differently Tyr-phosphorylated proteins identified in ChAc RBCs

Band no.	AC	Protein	Lyn-target	Score
1	P11277	β-spectrin (SPTB1)	Y-307*	2.447
			Y-474	3.596
			Y-493	3.383
			Y-660	4.128
			Y-1590*	3
2	P16157	Ankyrin (ANK1)	Y-884	3.83
			Y-1468	2.362
			Y-1750	2.447
3	Q8WX82	β-I spectrin form β I σ 3 (fragment) (Q8WX82)	Y-307*	2.447
			Y-474	3.596
			Y-493	3.383
			Y-660	4.128
			Y-1590*	3
4	P027330	Band 3 anion transport protein (B3AT)	Y-8	8.809
			Y-21	6.553
			Y-46	4.149
			Y-359	4.702
			Y-904	5.915
5	P027330	Band 3 anion transport protein (B3AT)	Y-8	8.809
			Y-21	6.553
			Y-46	4.149
			Y-359	4.702
			Y-904	5.915
6	Q9H4B4	Serine threonine protein kinase PLK3 (PLK3)	Y-136	2.383
7	P35612	β-adducin (ADDB)	Y-377*	0.66
8	P11171	Band 4.1 (EPB41)	Y-374	2.489
9	P16452	Band 4.2 (EPB42)	Y-435	2.085
10	Q9H4B4	Serine threonine protein kinase PLK3 (PLK3)	Y-136	2.383
11	Q00013	55-kDa erythrocyte membrane protein (EM55)	Y-331	2.468
			Y-429	2.83
12	Q00013	55-kDa erythrocyte membrane protein (EM55)	Y-331	2.468
			Y-429	2.83
13	P47895	Aldehyde dehydrogenase family 1 member A3 (AL1A3)	Y-497	1.683†
14	P04040	Catalase (CATA)	Y-260	1.809
15	O94921	Serine threonine protein kinase PFTAIRE-1 (CDK14	Y-135	4.17
16	Q14012	Calcium calmodulin-dependent protein kinase type 1 (KCC1A)	Y-20	2.872
			Y-235	2.723
17	P60709	β-actin (ACTB)	Y-240	2.702
18	Q96GD4	Serine threonine protein kinase 12 (AURKB)	Y-8	2.319
19	P04406	Glyceraldehyde-3-P-dehydrogenase (G3P)	Y-255	1.66†
20	P27105	Stomatin (STOM)	Y-60	0.213‡
			Y-123	0.404‡
			Y-124	0.234‡
			Y-252	0.426‡
21	P00918	Carbonic anhydrase 2 (CAH2)	Y-40	1.511†
			Y-51	1.745†
			Y-114	1.681†
22	Q96E17	Ras related protein Rab-3C (RAB3C)	Y-17	0.809‡
			Y-29	0.383‡
			Y-50	0.298‡
			Y-92	0.638‡
			Y-99	0.596‡
			Y-100	0.638‡
			Y-110	0.191‡
			Y-131	0.234‡

*Identified phosphopeptides of β-spectrin and β-adducin.
†Low threshold analysis.
‡Very low threshold analysis.

ChAc membrane by the addition of GST-Lyn/SH2 or the phosphorylated cytoplasmic domain of band 3. This suggests the unmasking of the Lyn domain on band 3, which allows Lyn to bind independently from the action of Syk. The conspicuous increase in Tyr phosphorylation state of ChAc RBC membrane proteins by exogenous Lyn supports this hypothesis.

Bioinformatic analyses show that in large part the differentially Tyr-phosphorylated proteins identified in ChAc indeed contain

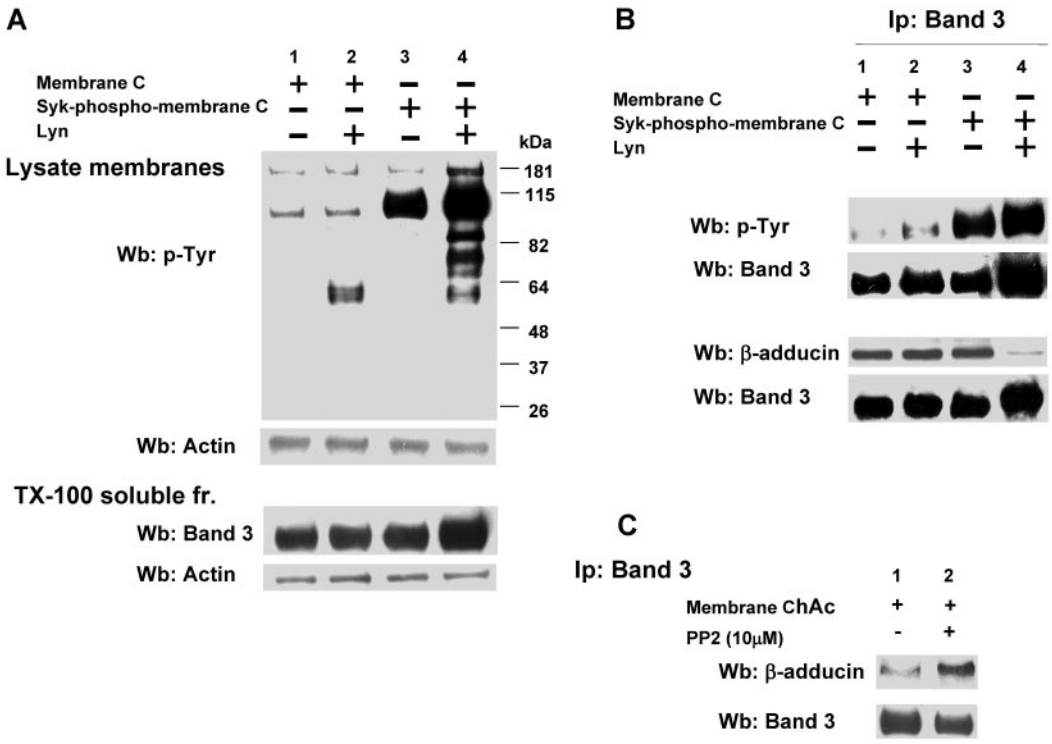

Figure 6. Effect of phosphorylation of RBC membranes by Syk and/or Lyn on band 3 binding to β-adducin in normal and ChAc RBC membranes. (A) Membranes (lanes 1 and 2) or Syk-phospho-membranes (lanes 3 and 4) of F2 RBCs from control (C) were incubated without (lanes 1 and 3) or with exogenous Lyn (lanes 2 and 4) and subjected to Western blot analysis with anti–phospho-Tyr (anti–pTyr) antibody (top panel) or were extracted with Triton X-100 and assayed after ultracentrifugation for the presence of band 3 by Western blot analysis (bottom panel). The membranes were reprobed with anti–actin antibody as loading control. (B) Band 3 was immunoprecipitated from membranes (lanes 1 and 2) and Syk-phospho-membranes (lanes 3 and 4) of F2 RBCs from C after incubation without (lanes 1 and 3) or with exogenous Lyn (lanes 2 and 4). The immunoprecipitates were subjected to Western blot analysis with anti–pTyr (top panel), anti–β-adducin antibody. The blots were also probed with anti–band 3 antibody. (C) Band 3 was immunoprecipitated from membranes of F2 ChAc RBCs previously incubated without or with the inhibitor PP2 (10μM). The immunoprecipitates were subjected to Western blot analysis with anti–β-adducin antibody. The blots were also probed with anti–band 3 antibody. The figure is representative of 3 independent experiments.

Lyn-specific targets or putative Src kinase family substrates. In addition, the sequence-structure study allowed us to propose specific Lyn phosphorylation sites on β-adducin and β-spectrin, supporting the multitarget action of abnormally activated Lyn in ChAc RBCs. Notably, Tyr-377 of β-adducin, which is phosphorylated in ChAc RBCs, is highly conserved.[36] This residue is located in the neck region that is involved in association of adducin monomers to heterodimers, thereby constituting the functionally active form of the protein. This conserved sequence in the neck region of adducin is also involved in the organization of an amphiphilic structure, which is important in mediating protein-protein interactions.[39] In ChAc RBCs, β-adducin was coimmunoprecipitated with band 3 only in the presence of the Src kinase inhibitor PP2, whereas in control erythrocytes there was a requirement for sequential Syk-Lyn band 3 phosphorylation. Thus, changes in the Tyr phosphorylation state of β-adducin in this region probably affect its interactions with the other proteins of the junctional complexes and thereby the stability of the RBC membrane protein bridges.

Our data suggest a novel mechanism in generation of acanthocytes in ChAc in addition to those reported in McLeod syndrome, a neuroacanthocytosis-related disorder, and in abetalipoproteinemia. In these diseases, acanthocytes formation has been related to either the absence of the XK membrane protein convalently linked to the Kell glycoprotein and part of the multiprotein 4.1 juctional complex as in McLeod syndrome or to the abnormal membrane lipid composition (increased sphingomielin/lecithin ratio) with abnormalities of lipid-lipid interaction within membrane as in abetaliproteinemia.[40,41] In ChAc RBCs, there is no indication of abnormalities in either membrane lipid composition or membrane and cytoskeletal protein content. We did, however, find alterations in Tyr-phosphorylation state of membrane proteins and in the signal transduction pathway. Thus, we propose that in ChAc RBCs the "Lyn storm" might affect the organization of the complexes bridging the membrane to the cytoskeleton, most likely by inducing abnormal protein interactions through the opening of SH2 binding sites in a Syk-independent manner. This might result in the heterogeneous distribution of the cytoskeleton as observed in electron microscopy studies,[8] and may be similar to the concentration of Lyn in plasma membrane patches of activated platelets, adjacent to granules.[42,43] In addition, abnormal Lyn phosphorylation might also contribute to altered vesiculation of ChAc RBCs. Lyn has been found in association with the exosomes that are excreted by reticulocytes, containing lipid raft domains, and in vesicles from mature RBCs.[44-46] Together with the indication for a stomatin-specific, raft-based process in vesicle formation in vitro,[47] this supports the hypothesis that vesicle formation is an important, active process in the formation of acanthocytes. This is in agreement with increased concentrations in ChAc RBC membranes of various small G-proteins involved in vesicle formation and transport.[10]

In conclusion, our data link, for the first time, the presence of abnormal RBCs in patients with ChAC with evidence for an independent and strong Lyn activation. The ChAc-associated alterations in RBC membrane-protein organization appear to be the result of increased Tyr phosphorylation leading to altered linkage

of band 3 to the junctional complexes involved in anchoring the membrane to the cytoskeleton. The latter may promote an increased degree of freedom of the junctional complexes bridging the membrane to the cytoskeleton and affect the association of the cytoskeleton with the plasma membrane. The present data open new ways to explore the pathobiology of acanthocytes and pathophysiologic mechanisms of neurodegeneration in patients with neuroacanthocytosis.

Acknowledgments

This work was supported by the Advocacy for Neuroacanthocytosis Patients (B.B., P.H.B.-G., E.L., G.J.C.G.M.B., and L.D.F.), Carl H. and Elizabeth S. Pforzheimer III, New York (B.B., P.H.B.-G., E.L., G.J.C.G.M.B., and R.H.W.), Ginger and Glenn Irvine, London (P.B., E.L., and G.J.C.G.M.B.) and Telethon (grant GPP07007, L.D.F.). Preliminary data were generated by Dr Christan Pozzobon.

Authorship

Contribution: L.D.F. and G.J.C.G.M.B. designed the experiments and analyzed the data; N.M. designed the study and wrote the manuscript; C.T., L.D.F., G.J.C.G.M.B., P.H.B.-G., A.S., and A.M. performed the experiments; M.B. performed the protein structure analysis and wrote the manuscript; A.M.B. and E.T. performed part of the Lyn analysis, analyzed the data, and wrote the manuscript; A.D., R.H.W., H.H.J., and B.B. performed neurologic diagnosis; A.D., B.B., R.H.W., and H.H.J. provided blood samples and confirmed diagnosis; E.F. performed part of the analysis by mass spectrometry; E.L. and C.T. performed bioinformatic analysis of the proteomic data; and all authors reviewed the manuscript.

Conflict-of-interest disclosure: The authors declare no competing financial interests.

Correspondence: Lucia De Franceschi, Department of Medicine, University of Verona, P.le L Scuro, 10, 37134 Verona, Italy; e-mail: lucia.defranceschi@univr.it.

References

1. Danek A, Jung HH, Melone MA, Rampoldi L, Broccoli V, Walker RH. Neuroacanthocytosis: new developments in a neglected group of dementing disorders. *J Neurol Sci.* 2005;229–230: 171-186.
2. Danek A, Walker RH. Neuroacanthocytosis. *Curr Opin Neurol.* 2005;18(4):386-392.
3. Jung HH, Danek A, Frey BM. McLeod syndrome: a neurohaematological disorder. *Vox Sang.* 2007; 93(2):112-121.
4. Rampoldi L, Danek A, Monaco AP. Clinical features and molecular bases of neuroacanthocytosis. *J Mol Med.* 2002;80(8):475-491.
5. Velayos-Baeza A, Levecque C, Dobson-Stone C, Monaco AP. The function of chorein. In: Walker RH, Saiki S, Danek A, eds. *Neuro-acanthocytosis Syndromes II*. Berlin, Germany: Springer-Verlag; 2008:87-105.
6. Dobson-Stone C, Velayos-Baeza A, Filippone LA, et al. Chorein detection for the diagnosis of chorea-acanthocytosis. *Ann Neurol.* 2004;56(2):299-302.
7. Mohandas N, Gallagher PG. Red cell membrane: past, present, and future. *Blood.* 2008;112(10): 3939-3948.
8. Terada N, Fujii Y, Ueda H, et al. Ultrastructural changes of erythrocyte membrane skeletons in chorea-acanthocytosis and McLeod syndrome revealed by the quick-freezing and deep-etching method. *Acta Haematol.* 1999;101(1):25-31.
9. Clark MR, Aminoff MJ, Chiu DT, Kuypers FA, Friend DS. Red cell deformability and lipid composition in two forms of acanthocytosis: enrichment of acanthocytic populations by density gradient centrifugation. *J Lab Clin Med.* 1989;113(4): 469-481.
10. Bosman GJCGM, de Franceschi L. Neuroacanthocytosis-related changes in erythrocyte membrane organization and function. In: Walker RH, Saiki S, Danek A, eds. *Neuroacanthocytosis syndromes II*. Berlin, Germany: Springer; 2008.
11. Olivieri O, De Franceschi L, Bordin L, et al. Increased membrane protein phosphorylation and anion transport activity in chorea-acanthocytosis. *Haematologica.* 1997;82(6):648-653.
12. Murthy SN, Wilson J, Zhang Y, Lorand L. Residue Gln-30 of human erythrocyte anion transporter is a prime site for reaction with intrinsic transglutaminase. *J Biol Chem.* 1994;269(36):22907-22911.
13. Melone MA, Di Fede G, Peluso G, et al. Abnormal accumulation of tTGase products in muscle and erythrocytes of chorea-acanthocytosis patients. *J Neuropathol Exp Neurol.* 2002;61(10):841-848.
14. Pasini EM, Kirkegaard M, Mortensen P, Lutz HU, Thomas AW, Mann M. In-depth analysis of the membrane and cytosolic proteome of red blood cells. *Blood.* 2006;108(3):791-801.
15. Bosman GJ, Lasonder E, Luten M, et al. The proteome of red cell membranes and vesicles during storage in blood bank conditions. *Transfusion.* 2008;48(5):827-835.
16. Bosman GJ, Willekens FL, Werre JM. Erythrocyte aging: a more than superficial resemblance to apoptosis? *Cell Physiol Biochem.* 2005;16(1):1-8.
17. Pasini EM, Lutz HU, Mann M, Thomas AW. Red blood cell (RBC) membrane proteomics: II. Comparative proteomics and RBC patho-physiology. *J Proteomics.* 2010;73(3):421-435.
18. Pasini EM, Lutz HU, Mann M, Thomas AW. Red blood cell (RBC) membrane proteomics: I. Proteomics and RBC physiology. *J Proteomics.* 2010;73(3):403-420.
19. De Franceschi L, Biondani A, Carta F, et al. PT-Pepsilon has a critical role in signaling transduction pathways and phosphoprotein network topology in red cells. *Proteomics.* 2008;8(22):4695-4708.
20. Siciliano A, Turrini F, Bertoldi M, et al. Deoxygenation affects tyrosine phosphoproteome of red cell membrane from patients with sickle cell disease. *Blood Cells Mol Dis.* 2010;44(4):233-242.
21. Bordin L, Ion-Popa F, Brunati AM, Clari G, Low PS. Effector-induced Syk-mediated phosphorylation in human erythrocytes. *Biochim Biophys Acta.* 2005;1745(1):20-28.
22. Matte A, Low PS, Turrini F, et al. Peroxiredoxin-2 expression is increased in beta-thalassemic mouse red cells but is displaced from the membrane as a marker of oxidative stress. *Free Radic Biol Med.* 2010;49(3):457-466.
23. Bosman GJ, Lasonder E, Groenen-Dopp YA, Willekens FL, Werre JM, Novotny VM. Comparative proteomics of erythrocyte aging in vivo and in vitro. *J Proteomics.* 2010;73(3):396-402.
24. van Gestel RA, van Solinge WW, van der Toorn HW, et al. Quantitative erythrocyte membrane proteome analysis with Blue-native/SDS PAGE. *J Proteomics.* 2010;73(3):456-465.
25. Donella-Deana A, James P, Staudenmann W, et al. Isolation from spleen of a 57-kDa protein substrate of the tyrosine kinase Lyn: identification as a protein related to protein disulfide-isomerase and localisation of the phosphorylation sites. *Eur J Biochem.* 1996;235(1):18-25.
26. Trentin L, Frasson M, Donella-Deana A, et al. Geldanamycin-induced Lyn dissociation from aberrant Hsp90-stabilized cytosolic complex is an early event in apoptotic mechanisms in B-chronic lymphocytic leukemia. *Blood.* 2008;112(12):4665-4674.
27. Brunati AM, Bordin L, Clari G, et al. Sequential phosphorylation of protein band 3 by Syk and Lyn tyrosine kinases in intact human erythrocytes: identification of primary and secondary phosphorylation sites. *Blood.* 2000;96(4):1550-1557.
28. Xue Y, Ren J, Gao X, Jin C, Wen L, Yao X. GPS 2.0, a tool to predict kinase-specific phosphorylation sites in hierarchy. *Mol Cell Proteomics.* 2008; 7(9):1598-1608.
29. Pantaleo A, De Franceschi L, Ferru E, Vono R, Turrini F. Current knowledge about the functional roles of phosphorylative changes of membrane proteins in normal and diseased red cells. *J Proteomics.* 2010;73(3):445-455.
30. Ferru E, Giger K, Pantaleo A, et al. Regulation of membrane-cytoskeletal interactions by tyrosine phosphorylation of erythrocyte band 3. *Blood.* 2011;117(22):5998-6006.
31. De Franceschi L, Villa-Moruzzi E, Biondani A, et al. Regulation of K-Cl cotransport by protein phosphatase 1alpha in mouse erythrocytes. *Pflugers Arch.* 2006;451(6):760-768.
32. Mallozzi C, De Franceschi L, Brugnara C, Di Stasi AM. Protein phosphatase 1alpha is tyrosine-phosphorylated and inactivated by peroxynitrite in erythrocytes through the src family kinase fgr. *Free Radic Biol Med.* 2005;38(12): 1625-1636.
33. Ipsaro JJ, Huang L, Gutierrez L, MacDonald RI. Molecular epitopes of the ankyrin-spectrin interaction. *Biochemistry.* 2008;47(28):7452-7464.
34. Ipsaro JJ, Harper SL, Messick TE, Marmorstein R, Mondragon A, Speicher DW. Crystal structure and functional interpretation of the erythrocyte spectrin tetramerization domain complex. *Blood.* 2010; 115(23):4843-4852.
35. Ipsaro JJ, Mondragon A. Structural basis for spectrin recognition by ankyrin. *Blood.* 2010; 115(20):4093-4101.
36. Matsuoka Y, Li X, Bennett V. Adducin: structure, function and regulation. *Cell Mol Life Sci.* 2000; 57(6):884-895.
37. Kolch W, Pitt A. Functional proteomics to dissect tyrosine kinase signalling pathways in cancer. *Nat Rev Cancer.* 2010;10(9):618-629.

38. Gauthier EGX, Mohandas N, An X. Phosphorylation-dependent perturbations of the 4.1R associated multiprotein complex of the erythrocyte membrane. *Biochemistry.* 2011;50(21):4561-4567.
39. Lupas A, Van Dyke M, Stock J. Predicting coiled coils from protein sequences. *Science.* 1991; 252(5009):1162-1164.
40. Cooper RA, Durocher JR, Leslie MH. Decreased fluidity of red cell membrane lipids in abetalipoproteinemia. *J Clin Invest.* 1977;60(1):115-121.
41. Salomao M, Zhang X, Yang Y, et al. Protein 4.1R-dependent multiprotein complex: new insights into the structural organization of the red blood cell membrane. *Proc Natl Acad Sci U S A.* 2008; 105(23):8026-8031.
42. Stenberg PE, Pestina TI, Barrie RJ, Jackson CW. The Src family kinases, Fgr, Fyn, Lck, and Lyn, colocalize with coated membranes in platelets. *Blood.* 1997;89(7):2384-2393.
43. Evangelista V, Pamuklar Z, Piccoli A, et al. Src family kinases mediate neutrophil adhesion to adherent platelets. *Blood.* 2007;109(6):2461-2469.
44. de Gassart A, Geminard C, Fevrier B, Raposo G, Vidal M. Lipid raft-associated protein sorting in exosomes. *Blood.* 2003;102(13):4336-4344.
45. Savina A, Vidal M, Colombo MI. The exosome pathway in K562 cells is regulated by Rab11. *J Cell Sci.* 2002;115(12):2505-2515.
46. Harder T, Scheiffele P, Verkade P, Simons K. Lipid domain structure of the plasma membrane revealed by patching of membrane components. *J Cell Biol.* 1998;141(4):929-942.
47. Salzer U, Zhu R, Luten M, et al. Vesicles generated during storage of red cells are rich in the lipid raft marker stomatin. *Transfusion.* 2008;48(3): 451-462.